*electronics*

*Article*

# An Optimal SVD Filtering Method for Measurement Accuracy Improvement against Harmonic Disturbance in Grid-Connected Inverters

**Hua Song, Yanbo Wang * and Xiang-E Sun ***

School of Electronics and Information, Yangtze University, Jingzhou 434025, China; 2021730055@yangtzeu.edu.cn
* Correspondence: wangyanbo@yangtzeu.edu.cn (Y.W.); xinges2000@yangtzeu.edu.cn (X.-E.S.)

**Abstract:** The increasing penetration of power electronics, such as grid-connected inverters and active loads may cause power quality issues, which reduce the sensitivity of monitoring and control systems due to measurement noises. This article presents an optimal singular value decomposition (SVD) filtering method for grid-connected inverters to improve sampling accuracy against measurement noises. First, the principle of this proposed method is based on the Hankel matrix theory, and then the implementation process is explained, during which the relationship between the Hankel matrix dimension and noise reduction is discussed. Furthermore, the optimal singular value is analyzed and proposed to determine the reconstruction order. Then, the comparative analysis of the proposed optimal SVD filtering method and difference spectrum method is given to explain the optimal reconstruction order. Finally, simulation verifications are implemented to validate the effectiveness of the proposed filtering method, considering the Hankel matrix dimension, reconstruction order, and different signal–noise ratio (SNR). The verification results show that the proposed optimal SVD filtering method can accurately identify the sampling current of grid-connected inverters, even if severe harmonic noises and oscillation happen. The proposed method can reduce the effects of harmonic disturbance on measurement accuracy and control performance of grid-connected inverters, which can improve the robustness of grid-connected inverters.

**Keywords:** singular value decomposition (SVD); grid-connected inverter; reconstruction order; oscillation; harmonic disturbance; measurement noises



**Citation:** Song, H.; Wang, Y.; Sun, X.-E. An Optimal SVD Filtering Method for Measurement Accuracy Improvement against Harmonic Disturbance in Grid-Connected Inverters. *Electronics* **2024**, *13*, 4087. https://doi.org/10.3390/electronics13204087

Academic Editors: José Manuel Ribeiro Baptista and Tiago Pinto

Received: 9 September 2024
Revised: 2 October 2024
Accepted: 15 October 2024
Published: 17 October 2024



## 1. Introduction

The increasing penetration of power electronic converters in renewable energy systems, such as wind power, electric vehicles, active loads, etc., poses important challenges in power quality, which further cause electromagnetic interference [1], harmonics, and inter-harmonics [2–6]. Also, harmonic oscillation phenomena can be caused due to the interaction of grid-connected inverters and time-varying grid impedance [7–10], etc. The power quality issue and oscillation issue may mitigate the accuracy of sampling and detection systems so that the performance of control systems is deteriorated [11,12]. The analysis in [13] shows that harmonics and inter-harmonics significantly reduce the sensitivity of monitoring systems and affect signal collection due to unexpected noises.

In grid-connected inverters of renewable energy system, noises from harmonics and inter-harmonics can cause false readings and misinterpretations, which is difficult to accurately analyze and interpret the information for control decision making and system management. To address this challenge, significant efforts were made. For example, a sliding mode control strategy was proposed in [14], which is further improved to handle the harmonic distortions caused by uncontrolled rectifiers in [15]. And the system's nonlinear modelling is simplified by using harmonic analysis. Given these complexities, Figure 1 shows the diagram of harmonic and oscillation sources in power electronic-dominated renewable energy systems. It can be seen that the harmonics and resonance can be caused by nonlinear loads, switching dynamics,

active loads, etc. Furthermore, the data-driven operation and control of renewable energies, such as big data and artificial intelligence, etc. are becoming an important trend, such as energy management and predictive maintenance [16], which tend to rely on precise data sampling. Hence, the ability to ensure reliable signal sampling and interpretation is critical [17]. The noise reduction in harmonic signals is of great significance to ensure the safe and reliable operation of renewable energy systems [18–20].

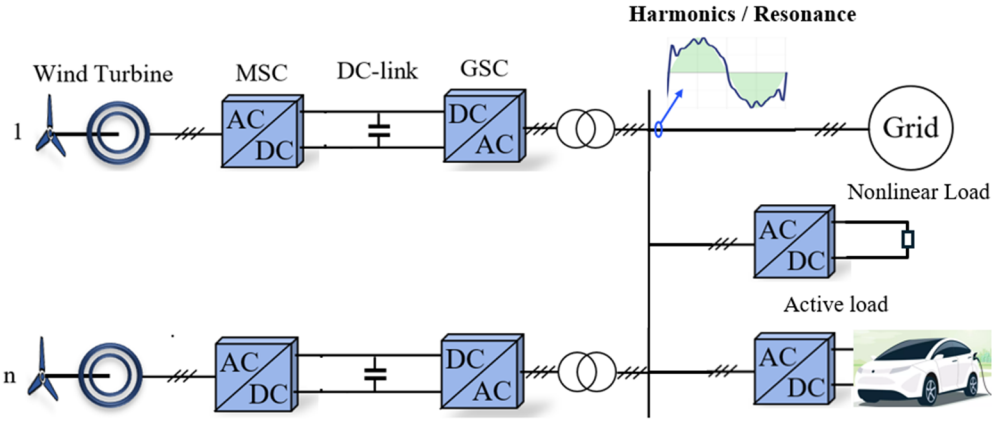


**Figure 1.** The diagram of harmonics and resonance sources in power electronic-dominated renewable energy system.

### *1.1. A Review of SVD-Based Noise Detection and Suppression Methods*

In modern electrical power systems, noise detection methods were previously proposed [21–32]. Singular value decomposition (SVD)-based methods were important solutions to realize noise detection and reduction [21]. In [22], singular spectrum analysis was employed to analyze the wind power series, which are decomposed into harmonic series and noise series. In [23], the SVD approach was used to selectively isolate characteristic parameters from a low-frequency voltage signal in electrical vehicles to obtain battery inconsistency data. In [24], singular value decomposition was adopted to remove narrowband interference in online partial discharge signals. A fault location method for MMC-HVDC system was developed in [25], which used a dichotomizing recursion SVD to pinpoint the arrival times of active pulses to determine the fault location in a modular multilevel converter high voltage direct current (MMC-HVDC) system. In [26], the SVD method was proposed to evaluate the dynamic virtual impedance on the virtual synchronous machine-based grid-connected inverter. In [27], high-impedance faults occurring on distribution lines were analyzed and detected by SVD. The aforementioned mathematic methods allow for the decomposition of a dataset into singular vectors and singular values, which can be used to effectively differentiate the signal and the noise components. The primary strength of SVD relies on its ability to identify and isolate the dominant patterns within the data, which are usually associated with the actual signal, while minimizing the less significant components attributed to noise [22,23].

The key problems in SVD are the selection of the Hankel matrix dimension and the determination of reconstruction order. In [28], it was proven that a singular value decomposition of a sample Hankel matrix can deal with the original signal as a linear superposition of a series of components. In [29], the difference spectrum was introduced to determine the sudden changes in singular values, allowing for the automatic selection of effective singular values. The analysis in [29] showed that selecting the appropriate number of rows and columns of the Hankel matrix can maximize noise removal. To determine the optimal reconstruction order, intensive studies were performed. In [30], a singular value ratio is used to determine the reconstruction order. Singular entropy was used to determine the truncation order in [31]. In [32], it was proved that the rank of the Hankel matrix is twice the number of effective frequency components, which provides theoretical guidance for the accuracy of the order determination method. Under the condition that the amplitude

difference in effective frequency components is too large, or the signal-to-noise ratio is low, the order determination results given by the existing methods were not consistent with the theoretical values. On this basis, fine tuning by manual order determination can realize satisfactory noise reduction performance. However, how to determine the reconstruction order in establishing a Hankel matrix should be further addressed.

### *1.2. New Contributions in This Work*

Although the singular value noise reduction technique based on the Hankel matrix was widely used in many fields of engineering, the dimensional structure and reconstruction order of the Hankel matrix can directly affect the noise reduction performance. Therefore, this article presents a new optimal SVD filtering method to reduce harmonic noise under background noises and systematically analyze effects of the dimensional structure and reconstruction order of the Hankel matrix, which is further applied in sampling noise filtering of grid-connected inverters against background harmonics. To compare with the previous work as listed in Table 1, the main contributions of this work are clarified as the following: (1) An innovative SVD filtering method is proposed to reduce harmonic noises, where the Hankel matrix construction method in the SVD process is proposed to select the optimal matrix dimension. (2) A new method to determine the reconstruction order is proposed. The proposed method can accurately identify the sampling current of a grid-connected inverter system, even if the severe harmonic noises and high-frequency oscillation phenomenon happen.

**Table 1.** A comprehensive comparison between previous research and this work.

| Reference | Adopted SVD Filtering Method | Applied Object | Effectiveness |
|---|---|---|---|
| [26] | SVD with Hankel matrix | Signal processing and noise reduction in vibration signals | Highly effective in signal decomposition, noise reduction, and singularity detection compared to wavelet transform |
| [27] | SVD with difference spectrum | Fault diagnosis in mechanical systems, specifically headstock | Highly effective in isolating fault-induced modulation features and noise reduction |
| [28] | SVD with singular value ratio spectrum | Extraction of fetal ECG from maternal ECG signal | Highly effective in separating maternal and fetal ECG components in real-time applications, despite noise interference |
| [29] | SVD with singular entropy theory | Noise reduction in structural vibration signals | Highly effective in improving signal-to-noise ratio |
| [30] | SVD with amplitude filtering characteristics | Fault diagnosis in rotating machinery, focusing on rotor vibrations | Highly effective in extracting key signal components and filtering noise, with zero-phase shift and high accuracy in identifying faults |
| This work | Optimal SVD filtering with Hankel matrix and reconstruction order optimization | Grid-connected inverters with harmonic disturbances | Highly effective in reducing harmonic and oscillation noise, improving signal sampling accuracy under severe noise conditions |

The rest of this article is organized as follows: In Section 2, the principle of singular value filtering is introduced. In Section 3, the principle and implementation process of the optimal SVD filtering method are proposed. In Section 4, a case study is given to validate the proposed optimal SVD filtering method, where the effectiveness of the proposed method is analyzed. The proposed method can reduce the effects of harmonic disturbance on measurement accuracy and further improve the robustness of grid-connected inverters. Finally, the conclusion is given in Section 5.

## 2. The Principle of Singular Value Filtering

The singular value filter, an effective filtering method, operates by mapping the original data onto a new set of bases that are determined from principal component analysis using singular value decomposition. Figure 2 shows the diagram of a singular value decomposition principle of a matrix, which is a factorization of any real or complex matrix A into a rotation, followed by a rescaling followed by another rotation. As illustrated in Figure 2, V* first rotates or reflects the input space. Then, Σ stretches or compresses the space along orthogonal axes. And U performs another rotation or reflection on the result, completing the SVD process.

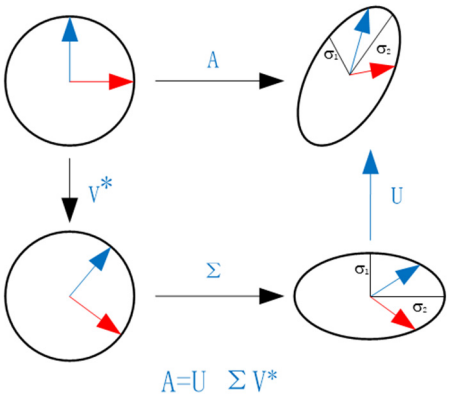


**Figure 2.** The diagram of singular value decomposition principle.

If a sampled signal $\widetilde{x}(n)$ is a linear superposition of $p$ harmonic and inter-harmonic signals, it can be represented as (1)

$$\widetilde{x}(n) = \sum_{i=1}^{p} a_i \cos(2\pi f_i n T_s + \varphi_i) \tag{1}$$

where $a_i$, $f_i$, $\varphi_i$, respectively, represent the amplitude, frequency, and initial phase of the $i$th signal component, and $T_s$ represent the sampling interval. Assuming that the noise $e(n)$ is white noise, the mean and variance are given as (2)

$$E[e(n)] = 0,\ D[e(n)] = \sigma^2 \tag{2}$$

Simultaneously, $e(n)$ is not correlated with the signal $\widetilde{x}(n)$, and $e(n)$ are not correlated as (3)

$$E(e(n_1)e(n_2)) = \begin{cases} 0, & n_1 \neq n_2 \\ \sigma^2, & n_1 = n_2 \end{cases} \tag{3}$$

Then, the model for collecting harmonic and inter-harmonic signals $x(n)$ under noise background can be represented as (4) from (1)

$$x(n) = \widetilde{x}(n) + e(n) = \sum_{i=1}^{p} a_i \cos(2\pi f_i n T_s + \varphi_i) + e(n) \tag{4}$$

The first step of the singular value filtering method is to construct the Hankel matrix. Assuming that the dimension of signal $x(n)$ is $N$, the Hankel matrix $\mathbf{H}$ with $m$ row and $l$ column is constructed using all the sample values $[x_0, x_1, \cdots x_{N-1}]$ as (5)

$$\mathbf{H} = \widetilde{\mathbf{H}} + \mathbf{E} = \begin{bmatrix} x_0 & x_1 & \cdots & x_{l-1} \\ x_1 & x_2 & \cdots & x_l \\ \vdots & \vdots & & \vdots \\ x_{m-1} & x_m & \cdots & x_{N-1} \end{bmatrix}_{m*l} \tag{5}$$

where $\widetilde{\mathbf{H}}$ is the Hankel matrix constructed for effective harmonic and inter-harmonic signals $\widetilde{x}(n)$, E is the Hankel matrix constructed for noise $e(n)$, and $m = N - l + 1$.

Then, a singular value decomposition is performed for the matrix H constructed from the signal $x(n)$ as (6).

$$\mathbf{H} = \widetilde{\mathbf{H}} + \mathbf{E} = \mathbf{U}\mathbf{\Sigma}\mathbf{V}^{\mathrm{T}} = \mathbf{U}\left[\begin{array}{c:c} \begin{matrix}\sigma_1 & & \\ & \ddots & \\ & & \sigma_\tau\end{matrix} & \mathbf{0} \\ \hdashline \mathbf{0} & \begin{matrix}\sigma_{\tau+1} & & \\ & \ddots & \\ & & \sigma_l\end{matrix} \\ \mathbf{0} & \mathbf{0} \end{array}\right]\mathbf{V}^T \tag{6}$$

where $\mathbf{U}$ and $\mathbf{V}$ are orthogonal matrices of $m \times m, l \times l$, respectively, and $\mathbf{\Sigma} = [\mathrm{diag}(\sigma_1, \sigma_2, \cdots \sigma_l);\ \mathbf{0}]$ is a diagonal matrix composed of the singular values of the matrix. $\mathbf{H}$ introduces the concept of subspace, assuming that the space $\mathbf{\Sigma}_\tau = \mathrm{diag}(\sigma_1, \sigma_2, \cdots \sigma_\tau)$, where the first $\tau$ singular values reside, corresponds to the signal subspace, and the space $\mathbf{\Sigma}_e = \mathrm{diag}(\sigma_{\tau+1}, \sigma_{\tau+2}, \cdots \sigma_l)$, where the remaining singular values reside, corresponds to the noise subspace. Then, the matrix $\hat{\mathbf{H}}$ is reconstructed with signal subspace $\mathbf{\Sigma}_\tau$.

$$\hat{\mathbf{H}} = \mathbf{U}_\tau \mathbf{\Sigma}_\tau \mathbf{V}_\tau^T \tag{7}$$

where $\mathbf{U_\tau}$ is the first $\tau$ column of matrix $\mathbf{U}$, and $\mathbf{V_\tau}$ is the first $\tau$ column of matrix $\mathbf{V}$. The effective signal $\widetilde{x}(n)$ without noises can be extracted by (7).

## 3. The Proposed Optimal Singular Value Filtering Method

### *3.1. The Principle of Optimal SVD Filtering Method*

According to the SVD singular value decomposition principle in Figure 2 and (7), the reconstruction matrix $\hat{\mathbf{H}}$ is the best approximation of the Hankel matrix $\widetilde{\mathbf{H}}$ of the effective signal $\widetilde{x}(n)$, which depends on how to construct the Hankel matrix and determine the reconstruction order $\tau$ based on the Hankel matrix. For the given $N$ samples $x(n)$, this work aims to select the optimal Hankel matrix dimension so that the singular value decomposition of sample matrix $\mathbf{H}$ in this dimension can minimize the influence of noise on the singular value of signal subspace. Then, the optimal reconstruction order $\tau$ is determined, so that the matrix $\mathbf{H}$ can realize the accurate separation of signal subspace and noise subspace according to the parameter.

The $m \times l$ Hankel matrix $\widetilde{\mathbf{H}}$ constructed by using the effective signal $\widetilde{x}(n)$ is represented as (8)

$$\widetilde{\mathbf{H}} = \begin{bmatrix} \widetilde{x}_0 & \widetilde{x}_1 & \cdots & \widetilde{x}_{l-1} \\ \widetilde{x}_1 & \widetilde{x}_2 & \cdots & \widetilde{x}_l \\ \vdots & \vdots & & \vdots \\ \widetilde{x}_{m-1} & \widetilde{x}_m & \cdots & \widetilde{x}_{N-1} \end{bmatrix} = \widetilde{\mathbf{U}}\widetilde{\mathbf{\Sigma}}\widetilde{\mathbf{V}} \tag{8}$$

According to [30], the relationship between the rank of matrix $\widetilde{\mathbf{H}}$ and the number of single frequency signals $p$ satisfies (9), when the number of columns $l$ of matrix $\widetilde{\mathbf{H}}$ is higher than twice $p$, that is, $l \geq 2p$.

$$R(\widetilde{\mathbf{H}}) = 2p \tag{9}$$

$A$ set ($A = \left\{\widetilde{\mathbf{H}} | l \geq 2p\right\}$) is built that contains all matrices $\widetilde{\mathbf{H}}$ with columns satisfying $l \geq 2p$ form, and the rank of all matrices in set $A$ is $2p$. The SVD of all matrices is constrained to the first $2p$ singular values in the matrix $\widetilde{\mathbf{\Sigma}}$, which provides a theoretical basis for the dimension optimization of the Hankel matrix.

For the $N$-point effective signal sequence $[\widetilde{x}_0, \widetilde{x}_1, \cdots, \widetilde{x}_{N-1}]$, it may be assumed that $N$ is odd (when $N$ is even, the endpoints are discarded), and the dimension of the Hankel

matrix $\widetilde{\mathbf{H}}$ is $m \times l$. When $m \geq l$, since $m = N - l + 1$, the number of columns of the matrix in set $A$ should meet (10)

$$2p \leq l \leq (N+1)/2 \tag{10}$$

when $m \leq l$, the row number of the new matrix after transposing the matrix $\widetilde{\mathbf{H}}$ is higher than the number of columns, and its singular values are unchanged so that it can be equivalent to the case of $m \geq l$.

The key problem to be solved by the Hankel matrix dimensional structure is to find the matrix $\widetilde{\mathbf{H}}_{opt}$ with the best noise reduction performance in set $A$, so that the effective signal has maximum energy representation, while the noise has minimum energy representation.

For this purpose, the matrix $\widetilde{\mathbf{H}}$ composed of $\widetilde{x}(n)$ containing $p$ single frequency signals is represented in a column vector form as (11).

$$\widetilde{\mathbf{H}} = \begin{bmatrix} \widetilde{\mathbf{x}}_0 & \widetilde{\mathbf{x}}_1 & \cdots & \widetilde{\mathbf{x}}_{l-1} \end{bmatrix} \tag{11}$$

where $\widetilde{\mathbf{x}}_i = \begin{bmatrix} \widetilde{x}_i & \widetilde{x}_{i+1} & \cdots & \widetilde{x}_{i+m-1} \end{bmatrix}^{\mathrm{T}}$ $(0 \leq i \leq l-1)$ represents a column vector consisting of $m$ consecutive sampling points starting from the $i$ sample point.

Define the singular value of matrix $\mathbf{H}$ ˜ as $(\widetilde{\sigma}_1, \widetilde{\sigma}_2, \cdots, \widetilde{\sigma}_l)$, then $(\widetilde{\sigma}_1^2, \widetilde{\sigma}_2^2, \cdots, \widetilde{\sigma}_l^2)$ is the eigenvalue of $\widetilde{\mathbf{H}}^T\widetilde{\mathbf{H}}$, and the relationship between the eigenvalue and the trace can be obtained as (12)

$$tr(\widetilde{\mathbf{H}}^T\widetilde{\mathbf{H}}) = \widetilde{\sigma}_1^2 + \widetilde{\sigma}_2^2 + \cdots + \widetilde{\sigma}_l^2 \tag{12}$$

It can be seen from (9) that only the first $2p$ terms of the singular value of matrix $\widetilde{\mathbf{H}}$ are non-zero so that Equation (12) is rewritten as (13)

$$tr(\widetilde{\mathbf{H}}^T\widetilde{\mathbf{H}}) = \widetilde{\sigma}_1^2 + \widetilde{\sigma}_2^2 + \cdots + \widetilde{\sigma}_{2p}^2 \tag{13}$$

From (11), $tr\left(\widetilde{\mathbf{H}}^T\widetilde{\mathbf{H}}\right)$ can be represented as (14)

$$\begin{aligned} tr(\widetilde{\mathbf{H}}^{\mathrm{T}}\widetilde{\mathbf{H}}) &= tr\left\{ \begin{bmatrix} \widetilde{\mathbf{x}}_0^{\mathrm{T}} \\ \widetilde{\mathbf{x}}_1^{\mathrm{T}} \\ \\ \widetilde{\mathbf{x}}_{l-1}^{\mathrm{T}} \end{bmatrix} \begin{bmatrix} \widetilde{\mathbf{x}}_0 & \widetilde{\mathbf{x}}_1 & \cdots & \widetilde{\mathbf{x}}_{l-1} \end{bmatrix} \right\} \\ &= tr\left\{ \begin{bmatrix} < \widetilde{\mathbf{x}}_0, \widetilde{\mathbf{x}}_0 > & < \widetilde{\mathbf{x}}_0, \widetilde{\mathbf{x}}_1 > & \cdots & < \widetilde{\mathbf{x}}_0, \widetilde{\mathbf{x}}_{l-1} > \\ < \widetilde{\mathbf{x}}_1, \widetilde{\mathbf{x}}_0 > & < \widetilde{\mathbf{x}}_1, \widetilde{\mathbf{x}}_1 > & \cdots & < \widetilde{\mathbf{x}}_1, \widetilde{\mathbf{x}}_{l-1} > \\ \vdots & \vdots & \ddots & \vdots \\ < \widetilde{\mathbf{x}}_{l-1}, \widetilde{\mathbf{x}}_0 > & < \widetilde{\mathbf{x}}_{l-1}, \widetilde{\mathbf{x}}_1 > & \cdots & < \widetilde{\mathbf{x}}_{l-1}, \widetilde{\mathbf{x}}_{l-1} > \end{bmatrix} \right\} \\ &= \sum_{i=0}^{l-1} < \widetilde{\mathbf{x}}_i, \widetilde{\mathbf{x}}_i > \end{aligned} \tag{14}$$

where $< \widetilde{\mathbf{x}}_i, \widetilde{\mathbf{x}}_i > = \sum_{j=0}^{m-1} \widetilde{x}_{i+j-1}^2$ is the inner product of the column vector $\widetilde{\mathbf{x}}_i$, representing the energy of the signal of that vector.

It can be derived by combining (13) and (14) as (15)

$$\begin{aligned} \widetilde{\sigma}_1^2 + \widetilde{\sigma}_2^2 + \cdots + \widetilde{\sigma}_{2p}^2 &= \sum_{i=1}^{l} < \widetilde{\mathbf{x}}_{\mathrm{i}}, \widetilde{\mathbf{x}}_{\mathrm{i}} > \\ &= \hat{x}_0^2 + 2\hat{x}_1^2 + \cdots + (l-1)\hat{x}_{l-2}^2 \\ &+ l\left(\hat{x}_{l-1}^2 + \hat{x}_l^2 + \cdots + \hat{x}_{N-l}^2\right) \\ &+ (l-1)\hat{x}_{N-l+1}^2 + \cdots + 2\hat{x}_{N-2}^2 + \hat{x}_{N-1}^2 \end{aligned} \tag{15}$$

Therefore, $tr\left(\widetilde{\mathbf{H}}^T\widetilde{\mathbf{H}}\right)$ characterizes the sum of energies of $l$ signals $\widetilde{\mathbf{x}}_i$ $(0 \le i \le l-1)$ of length $m$, and the problem of solving the optimal matrix $\widetilde{\mathbf{H}}_{opt}$ is converted to solve the trace maximization problem of matrix $\widetilde{\mathbf{H}}^T\widetilde{\mathbf{H}}$ as (16)

$$\begin{aligned} &\max_l(\widetilde{\sigma}_1^2+\widetilde{\sigma}_2^2+\cdots+\widetilde{\sigma}_{2p}^2) \\ &s.t\ \ 2p \le l \le (N+1)/2 \end{aligned} \tag{16}$$

For the fixed number of sampling points $N$, in the interval $2p \le l \le (N+1)/2$, $\widetilde{\sigma}_1^2+\widetilde{\sigma}_2^2+\cdots+\widetilde{\sigma}_{2p}^2$ increases monotonically with respect to $l$ so that the dimensionality of the optimal matrix $\widetilde{\mathbf{H}}_{opt}$ column can be represented as (17)

$$l = (N+1)/2 \tag{17}$$

The energy distribution of white noise $e(n)$ under the condition of Equation (16) is analyzed. The spectrum of white noise is full band equivalent distribution, and all frequency components contribute the same degree to noise $e(n)$. Therefore, all singular values $\sigma_{ei}$ of the Hankel matrix constructed by noise $e(n)$ are equal. When $l = (N+1)/2$, $l$ is the maximum value satisfying the construction of the Hankel matrix, so each singular value $\sigma_{ei}$ $(0 \le i \le l-1)$ is the minimum value, the noise is the minimum sum of squares of the first $2p$ singular values, and the noise energy is reduced to the lowest value in the reconstruction scale.

Therefore, when a Hankel matrix of size $m \times l$ is constructed with dimension $l = (N+1)/2$, the energy of signal $\widetilde{x}(n)$ is constrained to the first $2p$ singular values in $\widetilde{\mathbf{\Sigma}}$ matrix, while the energy of noise $e(n)$ at the first $2p$ singular values is reduced to the lowest value.

### *3.2. The Effects of Reconstruction Order*

Determination of the reconstruction order is a critical step. In [27], a singular value difference spectrum method is proposed to estimate the reconstruction order, which is often smaller than the actual reconstruction order when the amplitude of the frequency component has a certain difference.

On this basis, the singular threshold difference spectrum method is proposed by using the characteristic of noise power attenuation of 3 dB with double the number of sampling points, which is described as follows. For noise with a $-10$ db superposition of signals containing two effective frequency components, 1000, 2000, 4000, and 8000 sample points are, respectively, collected within the same interval length, and spectrum analysis is performed as shown in Figure 3.

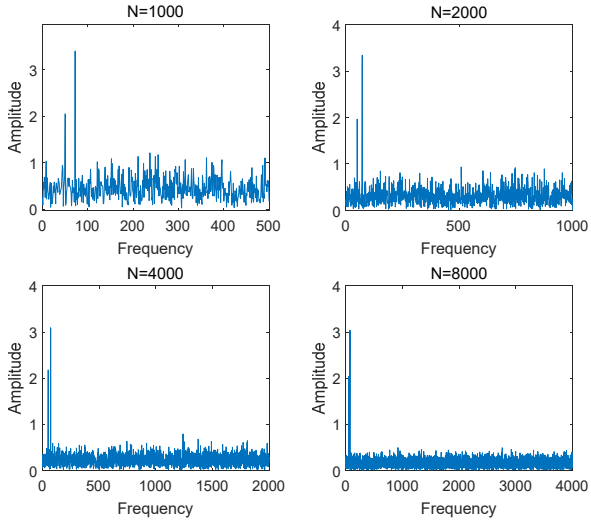


**Figure 3.** Frequency (Hz) multiplication sampling amplitude characteristics.

It can be seen from Figure 3 that, with the number increase in sampling points in a fixed interval, the amplitude of the effective frequency component has a small fluctuation, and the noise amplitude decreases significantly.

The amplitudes of $N$-point and $2N$-point noise are $(A_1, A_2, \cdots, A_N)$ and $(B_1, B_2, \cdots, B_{2N})$, respectively. Through a statistical analysis of the total power of noise frequency points, it is derived as (18)

$$\sum_{i=1}^{N} A_i^2 = \sum_{i=1}^{2N} B_i^2 \tag{18}$$

It shows that the total energy of noise in a fixed interval is constant. Assuming that the average powers of $N$-point and $2N$-point noise are $\overline{P}_N$ and $\overline{P}_{2N}$, it can be derived as $\overline{P}_N = \sum_{i=1}^{N} A_i^2/N$ and $\overline{P}_{2N} = \sum_{i=1}^{2N} B_i^2/2N$. Therefore, it can be represented as (19)

$$\overline{P}_{2N} = \frac{\overline{P}_N}{2} \tag{19}$$

This equation means that the average power of the noise can be decreased by 3 dB if the number of sampling points is doubled. Then, the amplitude of the frequency spectrum can be decreased by $1/\sqrt{2}$.

The analysis in [30] shows that if the amplitude of a certain frequency in the amplitude spectrum is larger, the corresponding two singular values will become higher, which will inevitably produce an obvious jump between the singular value of noise and the singular value of the active component, and the singular value of noise will become flatter. The above results indicate the principle of the reconstruction order determination. In other words, for a certain threshold, the sampling number is increased by a multiple of two until the singular value of the noise is lower than the threshold value, and the singular value of the effective frequency component is significantly higher than the threshold value.

The specific steps for reconstruction order determination for singular value decomposition (SVD) are clarified as follows:

(1) Select the initial sample number $N$, and construct the sample matrix with the optimal dimension $l = (N+1)/2$:

$$\mathbf{H} = \begin{bmatrix} x_0 & x_1 & \cdots & x_{(N-1)/2} \\ x_1 & x_2 & \cdots & x_{(N+1)/2} \\ \vdots & \vdots & & \vdots \\ x_{(N-1)/2} & x_{(N+1)/2} & \cdots & x_{N-1} \end{bmatrix} \tag{20}$$

(2) Perform singular value decomposition $\mathbf{H} = \mathbf{U}\mathbf{\Sigma}\mathbf{V}^T$ for the sample matrix $\mathbf{H}$ in (20), where the diagonal matrix $\mathbf{\Sigma} = \mathrm{diag}(\sigma_1, \sigma_1, \cdots \sigma_{(N+1)/2})$ is used to calculate the singular value difference spectrum as (21)

$$\varsigma_i = \sigma_i - \sigma_{i+1}, \quad 1 \le i \le (N-1)/2 \tag{21}$$

Given the threshold parameter $\varsigma$, the set $D = \{\varsigma_{\hat{l}} | \varsigma_{\hat{l}} > \varsigma\}$ containing spectral components greater than $\varsigma$ is built. And the reconstruction order $\tau$ should satisfy (22)

$$\tau = \max\{Index(\varsigma_i)\}, \ \varsigma_i \in D \tag{22}$$

where $Index(\varsigma_i)$ means the subscript $i$ of $\varsigma_i$; and $\max\{Index(\varsigma_i)\}$ means taking the largest $i$ value of all $\varsigma_i \in D$ subscripts as the estimate of the reconstruction order $\tau$.

(3) Then, increase the number of sample points to $2N$, and repeat steps 1–3. If the obtained reconstruction order $\tau$ changes, the number of sample points can be increased to $4N$, until the reconstruction order $\tau$ obtained by each calculation is constant.

### *3.3. Filtering Error Analysis*

To measure the noise reduction effect of singular value decomposition, this paper introduces the overall relative error $q$ as an evaluation index, which is normalized by solving the total error energy of the filtered curve and the reference curve. It is represented as (23)

$$q = \frac{\sum_{i=0}^{N-1} [\hat{x}(i) - x_c(i)]^2}{\sum_{i=0}^{N-1} x_c^2(i)} \tag{23}$$

where $\hat{x}(i)$ is the filtered data, and $x_c(i)$ is ideal data.

## 4. Case Study

To validate the performance of the proposed SVD filtering method of grid-connected inverters against harmonics and resonance, the case studies are implemented considering different harmonics, oscillation, and noise strength. Figure 4 shows the diagram of the grid-connected inverter system with the proposed SVD filtering method. In practical operation, the sampled voltage and current of the inverter can be disturbed by sampling noises due to background harmonics, sampling circuit ageing, high-frequency oscillation, etc.

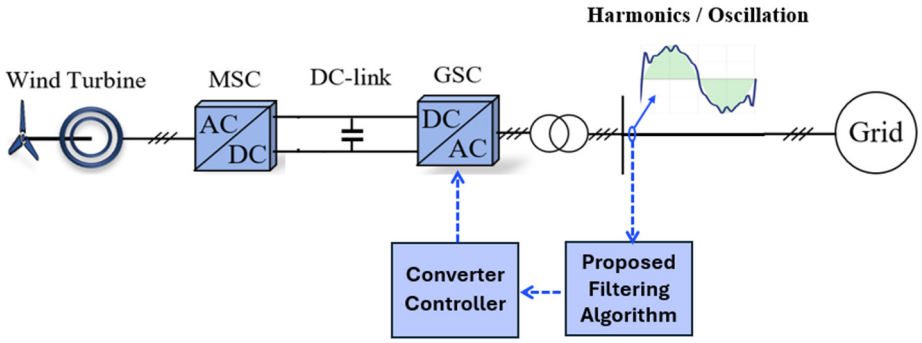


**Figure 4.** The diagram of a grid-connected inverter with the proposed SVD filtering method.

In this work, the grid-connected inverter in a wind turbine is adopted to exemplify the proposed method. A two-level PWM converter with an $L$ filter is applied in this grid-connected wind turbine. Figure 4 shows the diagram of a grid-connected inverter with the proposed SVD filtering method, where the current signals with harmonic and oscillation information should be accurately collected and feedbacked to the control system for harmonic and oscillation mitigation in practical operation.

### *4.1. Case I: Filtering Performance in Grid-Connected Inverters*

In long-term operation, harmonic noise amplification caused by sampling errors or parameter perturbations may weaken control system performance of grid-connected inverters. Especially under low-current operation, the sampling current is subject to harmonic noises or resonance. Thus, the proposed method aims to accurately identify the current from measurement noises and improve control system accuracy. In this case, the filtering performance under a different dimension of the Hankel matrix is validated. The current of the grid-connected inverter is disturbed with high-frequency sampling noises. The original current waveform with harmonic noises can be modelled as $x(t) = \cos((2\pi * 50)t + 60^\circ) + e(t)$, the sampling frequency is $f_s$ = 100 kHz, the sampling number is $N$ = 3999, and the SNR of the case study is 0 dB. The sample sequence is constructed with dimensions $l$ = 10, 100, 2000, respectively. The filtering performance of the proposed method in different dimensions are shown in Figure 5.

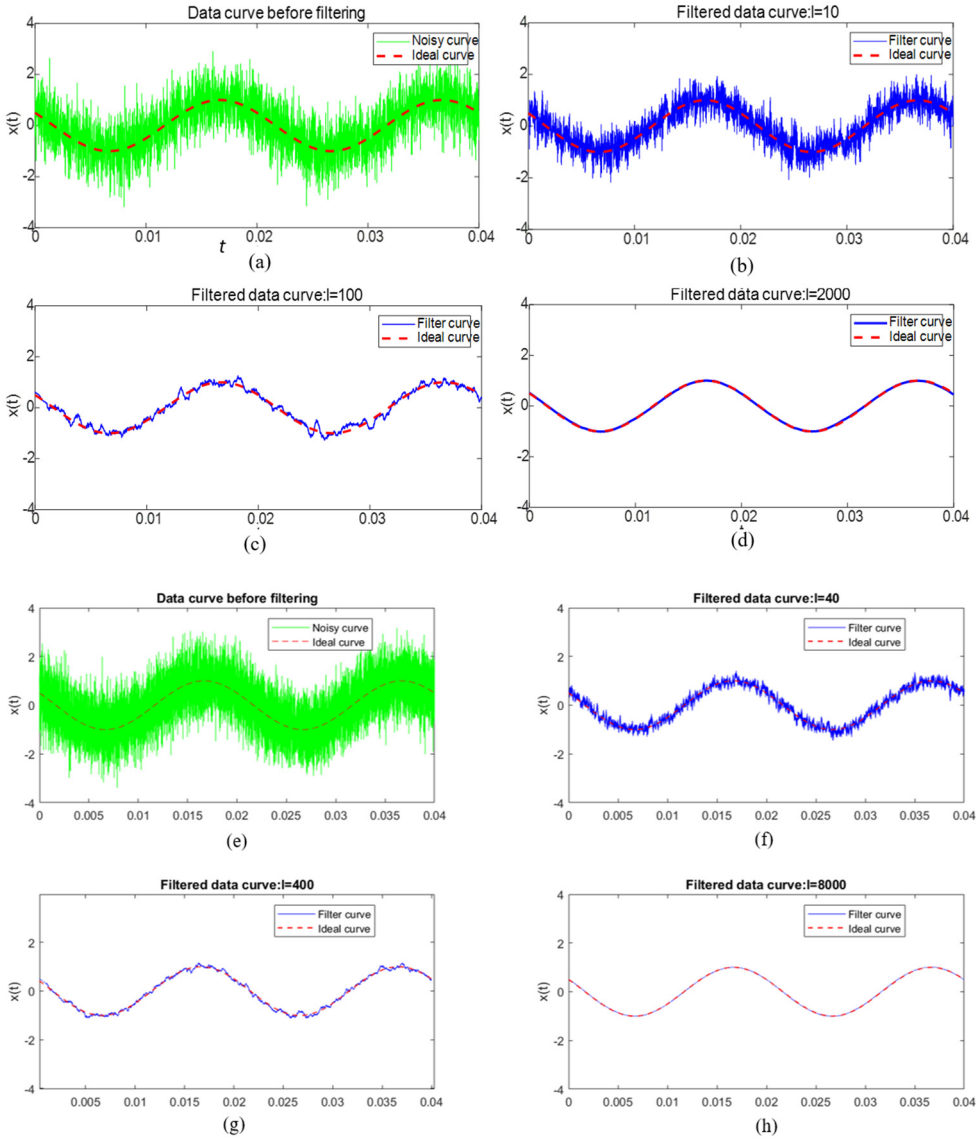


**Figure 5.** The verification results of the proposed method for sampling current of grid-connected inverters with sampling frequency of 100 kHz and 400 kHz. (**a**) Sampled current under 100 kHz. (**b**) Current with $l$ = 10, (**c**) Current with $l$ = 100, (**d**) Current with $l$ = 2000. (**e**) Sampled current under 400 kHz. (**f**) Current with $l$ = 40, (**g**) Current with $l$ = 400, (**h**) Current with $l$ = 8000.

Figure 5a shows a sampled current waveform before filtering, where the sampled current with noisy signals and ideal current are marked in green and red, respectively. Figure 5b–d shows the current of the grid-connected inverter by applying the proposed singular value filtering method with a sampling frequency of 100 kHz, where the filtering results of the Hankel matrix with different dimensions are shown. Under the same data sampling points, the overall relative error $q$ is 55.16%, 18.32%, and 2.51% when dimension $l$ is selected as 10, 100, and 2000, respectively. It means that the component size of noise in signal subspace can be suppressed as the increase in the Hankel matrix dimension. When dimension $l = (N + 1)/2 = 2000$, the optimal filtering result is realized, where the blue curve accurately matches the red curve.

To further validate the effectiveness of this proposed method in a grid-connected inverter based on wide bandgap devices with a high switching frequency, the higher sampling frequency $f_s$ = 400 kHz is given. Figure 5e shows a sampled current waveform before filtering, where the sampled current with noisy signals and ideal current are marked in green and red, respectively. Figure 5f–h shows the current of grid-connected inverters by

applying the proposed singular value filtering method with sampling frequency 400 kHz, where filtering results of the Hankel matrix with different dimensions are shown.

The verification results in Figure 5 show that the proposed method is applicable for grid-connected inverters with a sampling frequency of 400 kHz.

### *4.2. Case II: The Analysis for Reconstruction Order*

High-frequency oscillation issues of grid-connected inverters were reported in previous work [7–10]. The accurate sampling feedback of oscillations signals with high-frequency oscillation information is important for a control system to mitigate the high-frequency oscillation phenomena. This case aims to validate sampling capability of the proposed method against harmonic noises. When the high-frequency oscillation happens, the sampled current signal of the grid-connected inverter can be represented as (24).

$$\begin{aligned} x(t) \quad &= 10\cos((2\pi * 50)t + 60^\circ) \\ &+2\cos((2\pi * 150)t + 45^\circ) \\ &+2\cos((2\pi * 1000)t + 30^\circ) + e(t) \end{aligned} \tag{24}$$

The output current contains both integer multiple harmonics and inter-fractional harmonics, where the sampling frequency is $f_s$ = 100 kHz with the sampling number $N$ = 9999, and the signal-to-noise ratio in case study is 0 dB. The Hankel matrix is constructed with the sample sequence in dimension l = 5000, and the results of the singular value decomposition and difference spectrum calculation are shown in Figure 6.

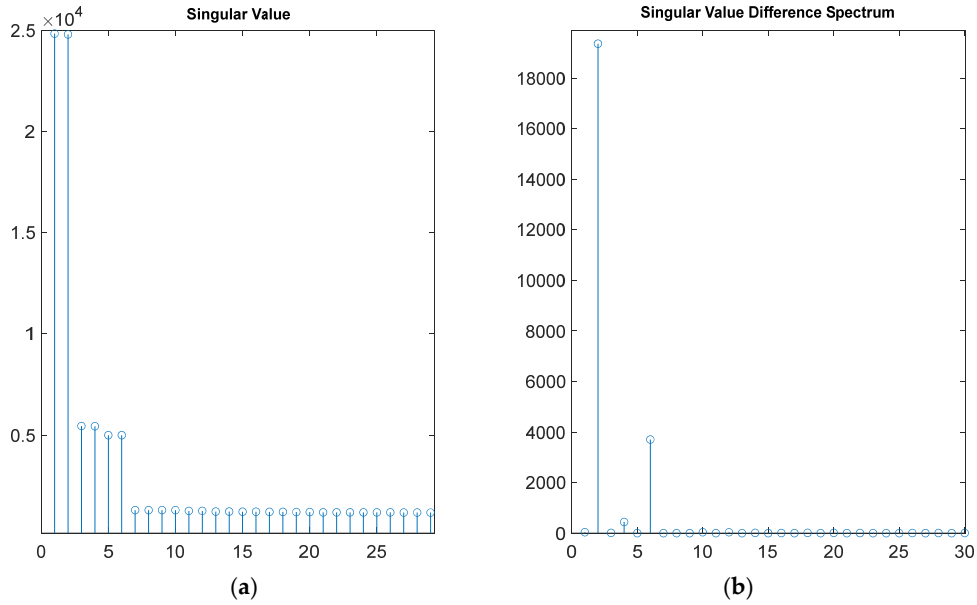


**Figure 6.** The results about singular value decomposition and difference spectrum calculation. (**a**) Singular value. (**b**) Singular value difference spectrum.

Figure 6 shows the calculation results of the first 25 singular values and their difference spectrum. It can be seen that the singular values show the characteristic of flat attenuation from the seventh serial number. Figure 6b shows the singular value difference spectrum method, where the maximum spectrum peak occurs at the serial number 2. Thus, the reconstruction order $\tau$ is given as two. Different from the difference spectrum method, the proposed method as shown in Figure 6a derives a serial number, where all the spectrum components at these serial numbers are higher than 100. Hence, the reconstruction order $\tau$ can be defined as six. It can be seen that the theoretical reconstruction order $\tau$ is six according to the relationship between frequency components and the rank of the Hankel matrix. However, the result given by the singular value difference spectrum method is

2-order. And the result given by the proposed method is consistent with the theoretical value.

Figure 7 shows the current sampling results of grid-connected inverters with different reconstruction order $\tau = 2$ and $\tau = 6$, respectively. Figure 7a shows the current sampling results under a difference spectrum calculation, where the reconstruction order is calculated as 2-order. It can be seen that the sampled current would be a sinusoidal waveform (blue curve), where the original high-frequency oscillation information is completely missing. It means that the sampling method under a difference spectrum calculation reduces the accuracy of the practical current, which fails to implement high-frequency oscillation detection and mitigation. Figure 7b shows the current sampling results under the proposed SVD filtering method, where the reconstruction order is defined as six orders. The sampled current (blue curve) accurately matches the practical current (red curve), where the high-frequency oscillation information can be completely detected and further used to design oscillation mitigation methods.

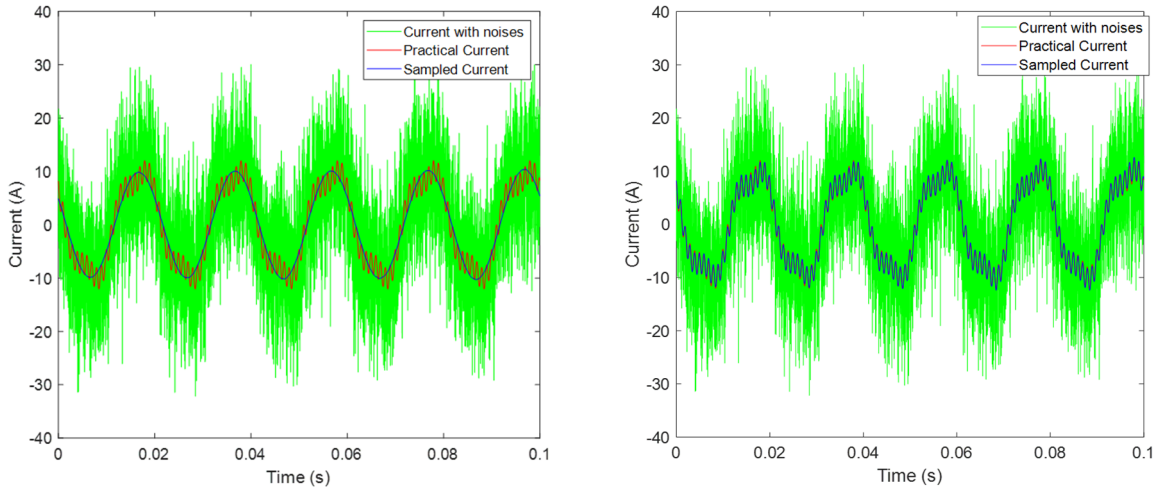


**Figure 7.** The sampled current of grid-connected inverter with different reconstruction methods. (**a**) The sampled current under difference spectrum calculation. (**b**) The sampled current under the proposed SVD filtering method.

This case study shows that the proposed SVD filtering method is able to accurately identify the inverter current with measurement noises even if a high-frequency oscillation phenomenon happens. And the high-frequency oscillation information can be accurately collected, which is important for oscillation suppression in a control system.

### *4.3. The Effect Analysis of Different Noise Strengths*

To further analyze the effects of different noise strengths, this case study is implemented, where the sinusoidal currents with different frequency and amplitudes are given. The sampled current signal of a grid-connected inverter can be represented as (25)

$$\begin{aligned} x(t) \quad &= 2.1\cos((2\pi * 50)t + 60^\circ) \\ &+2.5\cos((2\pi * 73)t + 45^\circ) \\ &+1.3\cos((2\pi * 83)t + 30^\circ) + e(t) \end{aligned} \tag{25}$$

The SNRs in this case study are given as 20 dB, 10 dB, 0 dB, and $-10$ dB, respectively. The sample sequence is constructed with dimension $l = 5000$ to establish the Hankel matrix. Figure 8 shows the sampled current under the proposed SVD filtering method in this work.

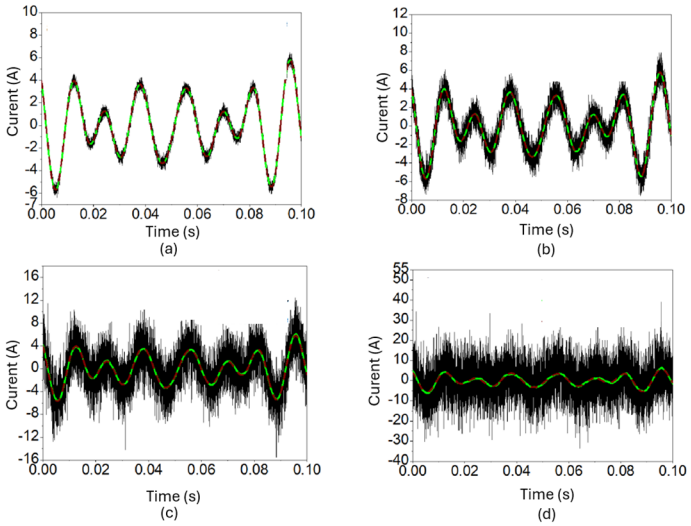


**Figure 8.** The sampled current with different SNRs under the proposed SVD filtering method. (**a**) SNR is 20 dB, (**b**) SNR is 10 dB, (**c**) SNR is 0 dB, and (**d**) SNR is −10 dB.

It can be seen from Figure 8 that with the reduction in signal-to-noise ratio, the practical current signal (red curve) can still be accurately collected from different noises, even if the extremely harsh noises with a SNR of −10 dB occurs (black curve). Hence, the proposed method exhibits a satisfied filtering performance under different noise strengths.

### *4.4. The Performance Analysis of Grid-Connected Inverters with Current Variation*

In practical operation, the current of a grid-connected inverter can be changed according to different nature features such as wind speed or solar irradiance. Figure 9 shows the current of a grid-connected inverter considering current variation, where the measurement noises deteriorate the signal sampling quality. It can be seen that the proposed SVD filtering method can accurately identify the sampled current (green curve) even if the inverter current is changed, where the current is decreased at 0.033 s and increased at 0.066 s to analyze the dynamic performance. This case validates the effectiveness of the proposed method under current variation.

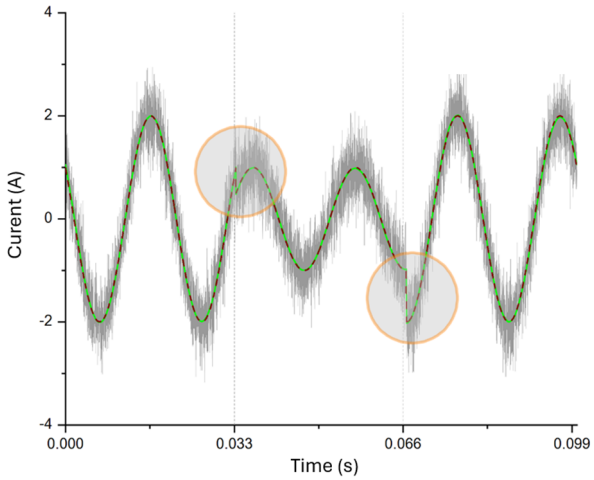


**Figure 9.** The current of a grid-connected inverter considering the dynamic performance of current variation.

Therefore, the above case studies show that the proposed SVD filtering method can accurately identify current signals in the presence of harmonic noises. In particular, the high-frequency oscillation information can be accurately captured in the presence of a grid

oscillation phenomenon, which is essential for the control system to damp the oscillation phenomenon and improve the robustness of grid-connected inverters in renewable energy generators. The availability of this proposed method in a large-scale wind power plant with multiple paralleled inverters will be further investigated in future work.

## 5. Conclusions

This article presents an optimal singular value decomposition (SVD) filtering method for grid-connected inverters to improve sampling accuracy in the presence of measurement noises. The principle of this method is first proposed based on the Hankel matrix theory. Furthermore, the effects of the matrix dimension and reconstruction order on SVD filtering results are analyzed. The case studies are given to validate the effectiveness of the proposed method. Also, the comparative analysis of the proposed optimal SVD filtering method and difference spectrum method is given to explain the optimal reconstruction order. This analysis shows that the proposed filtering method can accurately reconstruct the inverter current, especially high-frequency oscillation information, which can be identified in the presence of harmonic oscillation. Compared with the traditional difference spectrum method, a more accurate reconstruction order can be obtained by the proposed SVD filtering method, which can accurately reconstruct practical current signals of a grid-connected inverter in the presence of high-frequency oscillation, current variation, etc. The proposed optimal SVD filtering method can improve signal sampling accuracy of grid-connected inverters against harmonic disturbances, which is important for control system design and stability enhancement.

**Author Contributions:** Conceptualization, H.S. and Y.W.; methodology, X.-E.S.; software, H.S.; investigation, H.S. and Y.W.; writing—original draft preparation, H.S. and Y.W.; writing—review and editing, X.-E.S.; supervision, X.-E.S. All authors have read and agreed to the published version of the manuscript.

**Funding:** This research received no external funding.

**Data Availability Statement:** Data are contained within the article.

**Conflicts of Interest:** The authors declare no conflicts of interest.

## References

1. Charalambous, C.A.; Demetriou, A.; Lazari, A.L.; Nikolaidis, A.I. Effects of electromagnetic interference on underground pipelines caused by the operation of high voltage AC traction systems: The impact of harmonics. *IEEE Trans. Power Deliv.* **2018**, *33*, 2664–2672. [CrossRef]
2. Almutairi, M.S.; Hadjiloucas, S. Harmonics mitigation based on the minimization of non-linearity current in a power system. *Designs* **2019**, *3*, 29. [CrossRef]
3. Eroğlu, H.; Cuce, E.; Cuce, P.M.; Gul, F.; Iskenderoğlu, A. Harmonic problems in renewable and sustainable energy systems: A comprehensive review. *Sustain. Energy Technol. Assess.* **2021**, *48*, 101566. [CrossRef]
4. Shaik, A.G.; Mahela, O.P. Power quality assessment and event detection in hybrid power system. *Electr. Power Syst. Res.* **2018**, *161*, 26–44. [CrossRef]
5. Mishra, M. Power quality disturbance detection and classification using signal processing and soft computing techniques: A comprehensive review. *Int. Trans. Electr. Energy Syst.* **2019**, *29*, e12008. [CrossRef]
6. Fisher, M.E.; Sharaf, A.M. A continuous frequency optimization technique for power system harmonic filter design. *Eng. Optim.* **1994**, *23*, 71–86. [CrossRef]
7. Wang, Y.; Wang, X.; Chen, Z.; Blaabjerg, F. Small-signal stability analysis of inverter-fed power systems using component connection method. *IEEE Trans. Smart Grid* **2017**, *9*, 5301–5310. [CrossRef]
8. Ding, H.; Wang, J.T.; Lu, L.Q.; Pan, J.W. Parameter optimization of toroidal tuned liquid column dampers for suppressing multi-directional harmonic vibration of structures. *Eng. Optim.* **2022**, *54*, 1–19. [CrossRef]
9. Wang, Y.; Wang, X.; Blaabjerg, F.; Chen, Z. Harmonic instability assessment using state-space modeling and par-ticipation analysis in inverter-fed power systems. *IEEE Trans. Ind. Electron.* **2016**, *64*, 806–816. [CrossRef]
10. Cai, J.; Wang, M.Y.; Xia, Q.; Luo, Y. Optimal design of a tapping-mode atomic force microscopy cantilever probe with resonance harmonics assignment. *Eng. Optim.* **2017**, *49*, 43–59. [CrossRef]
11. Arranz-Gimon, A.; Zorita-Lamadrid, A.; Morinigo-Sotelo, D.; Duque-Perez, O. A review of total harmonic distortion factors for the measurement of harmonic and interharmonic pollution in modern power systems. *Energies* **2021**, *14*, 6467. [CrossRef]

12. George, J.W. *Power Systems Harmonics Fundamentals, Analysis and Filter Design*; Springer: Berlin/Heidelberg, Germany, 2001.
13. Wang, Y.; Li, Q.; Zhou, F.; Zhou, Y.; Mu, X. A new method with Hilbert transform and slip-SVD-based noise-suppression algorithm for noisy power quality monitoring. *IEEE Trans. Instrum. Meas.* **2018**, *68*, 987–1001. [CrossRef]
14. Canciello, G.; Cavallo, A.; Cucuzzella, M.; Ferrara, A. Fuzzy scheduling of robust controllers for islanded DC microgrids applications. *Int. J. Dyn. Control* **2019**, *7*, 690–700. [CrossRef]
15. Canciello, G.; Cavallo, A.; Guida, B. Robust control of aeronautical electrical generators for energy management applications. *Int. J. Aerosp. Eng.* **2017**, *2017*, 1745154. [CrossRef]
16. Qiu, Y.; Wang, Y.; Tian, Y.; Chen, Z. An Intelligent Stability Prediction Method of Grid-Connected Inverter Considering Time-varying Parameters. *IEEE Trans. Ind. Appl.* **2024**, *60*, 3685–3697. [CrossRef]
17. Santos, E.; Khosravy, M.; Lima, M.A.; Cerqueira, A.S.; Duque, C.A. ESPRIT associated with filter bank for power-line harmonics, sub-harmonics and inter-harmonics parameters estimation. *Int. J. Electr. Power Energy Syst.* **2020**, *118*, 105731. [CrossRef]
18. Gnaciński, P.; Pepliński, M.; Murawski, L.; Szeleziński, A. Vibration of induction machine supplied with voltage containing subharmonics and interharmonics. *IEEE Trans. Energy Convers.* **2019**, *34*, 1928–1937. [CrossRef]
19. Sangwongwanich, A.; Yang, Y.; Sera, D.; Soltani, H.; Blaabjerg, F. Analysis and modeling of interharmonics from grid-connected photovoltaic systems. *IEEE Trans. Power Electron.* **2018**, *33*, 8353–8364. [CrossRef]
20. Lopez, A.R.; López-Núñez, O.A.; Pérez-Zúñiga, R.; Gómez Radilla, J.; Martínez-García, M.; López-Osorio, M.A.; Ortiz-Torres, G.; Mena-Enriquez, M.G.; Ramos-Martinez, M.; Mixteco-Sánchez, J.C.; et al. Total Harmonic Distortion Reduction in Multilevel Inverters through the Utilization of the Moth–Flame Optimization Algorithm. *Appl. Sci.* **2023**, *13*, 12060. [CrossRef]
21. Khoshbin, F.; Bonakdari, H.; Ashraf Talesh, S.H.; Ebtehaj, I.; Zaji, A.H.; Azimi, H. Adaptive neuro-fuzzy inference system multi-objective optimization using the genetic algorithm/singular value decomposition method for modelling the discharge coefficient in rectangular sharp-crested side weirs. *Eng. Optim.* **2016**, *48*, 933–948. [CrossRef]
22. Wang, C.; Zhang, H.; Ma, P. Wind power forecasting based on singular spectrum analysis and a new hybrid Laguerre neural network. *Appl. Energy* **2020**, *259*, 114139. [CrossRef]
23. Jiang, J.; Zhang, R.; Wu, Y.; Chang, C.; Jiang, Y. A fault diagnosis method for electric vehicle power lithium battery based on wavelet packet decomposition. *J. Energy Storage* **2022**, *56*, 105909. [CrossRef]
24. Zhong, J.; Bi, X.; Shu, Q.; Chen, M.; Zhou, D.; Zhang, D. Partial discharge signal denoising based on singular value decomposition and empirical wavelet transform. *IEEE Trans. Instrum. Meas.* **2020**, *69*, 8866–8873. [CrossRef]
25. Bi, T.; Wang, S.; Jia, K. Single pole-to-ground fault location method for MMC-HVDC system using active pulse. *IET Gener. Transm. Distrib.* **2018**, *12*, 272–278. [CrossRef]
26. Rodríguez-Cabero, A.; Roldán-Pérez, J.; Prodanovic, M. Virtual impedance design considerations for virtual synchronous machines in weak grids. *IEEE J. Emerg. Sel. Top. Power Electron.* **2019**, *8*, 1477–1489. [CrossRef]
27. Chaitanya, B.K.; Yadav, A.; Pazoki, M. An intelligent detection of high-impedance faults for distribution lines integrated with distributed generators. *IEEE Syst. J.* **2019**, *14*, 870–879. [CrossRef]
28. Zhao, X.; Ye, B. Similarity of signal processing effect between Hankel matrix-based SVD and wavelet transform and its mechanism analysis. *Mech. Syst. Signal Process.* **2009**, *23*, 1062–1075. [CrossRef]
29. Zhao, X.; Ye, B. Selection of effective singular values using difference spectrum and its application to fault diagnosis of headstock. *Mech. Syst. Signal Process.* **2011**, *25*, 1617–1631. [CrossRef]
30. Kanjilal, P.P.; Palit, S.; Saha, G. Fetal ECG extraction from single-channel maternal ECG using singular value decomposition. *IEEE Trans. Biomed. Eng.* **1997**, *44*, 51–59. [CrossRef]
31. Jianwei, Z.; Huokun, L. Noise Reduction Technology of Random Vibration Signal Based on Singular Entropy Theory. In Proceedings of the 2009 Second International Symposium on Information Science and Engineering, Shanghai, China, 26–28 December 2009; IEEE: Piscataway, NJ, USA, 2009; pp. 32–35.
32. Guo, M.; Li, W.; Yang, Q.; Zhao, X.; Tang, Y. Amplitude filtering characteristics of singular value decomposition and its application to fault diagnosis of rotating machinery. *Measurement* **2020**, *154*, 107444. [CrossRef]